Research Square

Preprints are preliminary reports that have not undergone peer review.
They should not be considered conclusive, used to inform clinical practice,
or referenced by the media as validated information.

On springtails (Hexapoda: Collembola): A morphofunctional study of the jumping apparatus

Fábio G. L. Oliveira (fabio.oliveira@uni-rostock.de)
Universitat Rostock Mathematisch-Naturwissenschaftliche Fakultat https://orcid.org/0000-0001-6443-1967

Research Article

Keywords: Basal plates, Basal sclerites, Furca, Hemolymph pressure, Resilin, Retinaculum, Spring mechanism.

Posted Date: April 18th, 2022

DOI: https://doi.org/10.21203/rs.3.rs-1554131/v1

License: This work is licensed under a Creative Commons Attribution 4.0 International License.
Read Full License

Abstract

Background

Springtails (Hexapoda: Collembola) are tiny organisms that lead a hidden life, mostly occuring deep in the soil and on leaf litter. They have a variety of interesting body morphology patterns, the most famous of which is the catapult-like structure that enables them to jump and flee from predators. This highly specialized jumping apparatus consists of a mobile furca, which when at rest fits into a trigger, "the retinaculum" on the ventral side of the abdomen. Despite the many studies that have attempted to investigate the jumping apparatus, the actual mechanisms involved in the jump, for example the way in which the furca is released by the retinaculum, how and where the mechanisms of spring and hydrostatic pressure originate, are still not properly understood. The morphology of the jumping apparatus of *Orchesella cincta* was investigated in detail using confocal laser scanning microscopy and MicroCT techniques for 3D reconstruction.

Results

The morphology of *O. cincta* with both flexed and extended furca is analysed and described. The abdominal musculature involved in the jumping mechanism and relevant structures of the exoskeleton of retinaculum and furca are described in detail. With the data obtained in this study, hypotheses can be made about 1) where and how the spring and hydrostatic pressure mechanisms originate; 2) which muscles act on the extension and flexion of the furca; 3) which muscles act on the retinaculum and 4) how the retinaculum is released from the furca.

Conclusions

The comparative morphological study proved informative, and shows how springtail jumping involves mechanisms unique to this taxon. Hydrostatic pressure regulation possibly varies between animals with distinct segmentation, and those with fused segmentation. Interesting cuticular characters were revealed, such as basal plates and sclerites related to the construction of the spring mechanism. The present study establishes itself as a model option for future morphofunctional studies on springtails' jumping. Analysis of videos and images using a high speed camera will be useful for understanding how the jump develops through take-off, aerial and landing phases.

Background

Small animals like arthropods that perform fast movements such as predation and jumping depend on much greater limb accelerations than larger animals. To overcome the temporal limitations of muscle contraction, some arthropods developed, independently, a strategy for power amplification, the spring mechanism involving motors and latches. The spring mechanism enables the animal to store energy for

the desired movement and release it instantly when needed (Burrows 1969; Gronemberg 1996; Ilton et al. 2018).

Springtails are tiny hexapods (Collembola) (0.1-5.0 mm) that predominantly inhabit the surface layer of the ground and are commonly found on/among litter fragments (Eisenbeis & Wichard, 1987; Hopkin, 1997; Palacios-Vargas *et al.*2007; Rusek, 1998). One of the most remarkable features of these animals is their ability to jump in order to escape predators, a feat only made possible by a highly sophisticated device (Figs. 1A-B) (Sudo et al. 2013a, b). Describing it superficially, this apparatus is essentially composed of a propulsion organ, the furca, and a retinaculum where the furca is held until the moment of the jump.

Although the various mechanisms involved in the springtail jump have been addressed in previous studies, due to the scarcity of morphological evidence there are still questions which remain to be clarified. The muscular system in segmented springtails was described by Manton (1972) and Eisenbeis (1978), both studies using *Tomocerus longicornis* (Müller, 1776). Manton (1972) offered a morphofunctional interpretation of the jumping, while Eisenbeis (1978) took a more descriptive approach. Manton (1972), Eisenbeis & Ulmer (1978) and Christian (1979) all mentioned the basal sternites as important parts of the jumping apparatus, due to their mobility and elasticity. Manton (1972) and Christian (1979) described the basal sclerite of the 4th segment, as the “basal rods”, hypothesizing that the elastic energy required for the spring mechanism could be stored there. The mechanism that triggers the jump (releasing the spring) is the subject of a discussion that has not yet been resolved. Manton (1972) proposed that hydraulic pressure alone triggers the jump, but this was later refuted by Christian (1979), who believed the release of the spring was mainly the result of muscular action. Eisenbeis & Ulmer (1978) and Brackenbury & Hunt (1993) agreed that the two mechanisms (muscle system and hydraulic pressure) could act together or independently as a motive force to release the spring. However, our understanding of how and where these two different mechanisms originate? on a body systematic level is still preliminary.

The retinaculum and furca are, respectively, modified states of the ambulatory legs of the 3rd and 4th abdominal segments (Konopova & Akam, 2014) which diversified more than 400 MA (Whalley & Jarzembowski, 1981) into these two very unique structures that work together in an intersegmental relationship to facilitate the famous springtail jump. In addition to being the oldest, springtails are also the most abundant and widely distributed hexapods on the planet, occurring in most strata (horizontal and vertical distribution in the landscape). Their habitats include the forest canopy and soil surface, deeper layers of the soil, the surface of lakes, and even your home. As the soil depth at which they are found increases, a reduction in body size and a shortening of legs, antennae and furca can be observed (these can be also absent due to secondary loss) (Gisin, 1943). A wide range of body shapes are noted among springtails, according to the environment in which they live. At the same time, a high degree of convergence means that similarly shaped structures are found in taxa that do not have a close phylogenetic connection (Agolin & D’Haese, 2009). This diversity of morphological shapes and habitat use, the miniaturized body architecture (Panina et al. 2019) and the presence of appendages exclusively

used in jumping make springtails one of the most interesting model organisms for the study of spring mechanisms and jumping behavior in Arthropoda.

In this study, which uses confocal laser scanning microscopy (cLSM), MicroCT and 3D models, I describe the jumping apparatus of *Orchesella cincta* (Linnaeus, 1758), including the muscular system of the retinaculum and furca, and cuticular structures such as the tergites, basal sternites and elastic endosclerites of the abdomen, retinaculum and furca. This is the first comparative investigation into morphological shape in the "flexed furca" and "extended furca" phases, and it culminates in an interpretation and discussion of the morphofunctional mechanisms of the jump showing the main elements behind this phenomenon and explaining how and where the hydraulic pressure and spring mechanism potentially originate.

Results

The morphology of the jumping apparatus was studied comparatively between specimens of *Orchesella cincta* with extended and flexed furca (Figs. 2A-C). Abdominal segments 2–6 were reconstructed, including cuticular structures such as basal plates and sclerites, as well as internal musculature. The architecture of the abdomen in *Orchesella cincta* is defined by visible and clear segmentation. The 4th abdominal segment is longer than the others, with a well-developed furca which inserts ventrally. A complex muscular system with muscles oriented predominantly parallel to the longitudinal axis is characteristic in *O. cincta*. Recognizable at the base of the furca are the basal plates - mobile and elastic cuticular structures via which the furca articulates with the abdomen on a longitudinal axis. Three basal plates BP1, BP2 and BP3 are found ventrolaterally in the abdomen, connecting to each other at the edges. Their architecture, mobility and elasticity are intrinsically related to the jumping behavior. The movement of the basal plates and the abdominal segments occurs mainly by muscular action. The furca is extended via an anteroposteriorly oriented rotary movement capable of a 180º execution angle. When extended, the furca protrudes posteriorly and is highly exposed. When flexed, the furca folds ventrally together with the basal plates, hiding in the inner part of the abdomen while attached to the retinaculum (Figs. 3A-B, 4, 5A-B).

In the following, the form and functioning of the main parts of the jumping apparatus are described. An interpretation of the morphofunctional mechanisms is provided on the basis of a comparison between individuals with flexed and extended furca. MicroCT reconstructions of all muscles and the cuticular walls of the 2-6th abdominal segments can be found in Figs. 3A-B and 4. A descriptive list of reconstructed muscles and information about attachment points is provided below in Table 1.

Table 1

Table describing the muscles of 2nd -6th abdominal segments and their respective attachment points in *Orchesella cincta*.

Name of the muscle	origin	insertion point
M.IIa-dlm1	tergite of IIa anterior dorsal medial	tergite of IIIa anterior dorsal medial
M.IIa-dlm2	tergite of IIa anterior dorsal medial	tergite of IIIa anterior dorsal medial
M.IIa-dlm3	tergite of IIa anterior dorsal medial	tergite of IIIa anterior dorsal medial
M.IIa-llm1	tergite of IIa anterior lateral medial	tergite of IIIa anterior lateral medial
M.IIa-llm2	tergite of IIa anterior lateral medial	tergite of IIIa anterior lateral medial
M.IIa-llm3	tergite of IIa anterior lateral medial	tergite of IIIa anterior lateral medial
M.IIa-llm4	tergite of IIa anterior lateral medial	tergite of IIIa anterior lateral medial
M.IIa-llm5	tergite of IIa anterior lateral medial	tergite of IIIa anterior lateral medial
M.IIa-isdlm1	muscle centre dorsomedial in transition area between Ia and IIa	muscle center dorsolateral in transition area between IIIa and IVa
M.IIa-isdlm2	muscle centre dorsomedial in transition area between Ia and IIa	muscle center dorsolateral in transition area between IIIa and IVa
M.IIa-isllm1	muscle centre ventral lateral in transition area between IIa and IIIa	tergite of IIIa ventral lateral in transition area between IIIa and Iva
M.IIa-isllm2	muscle centre ventral lateral in transition area between IIa and IIIa	tergite of IIIa ventral lateral in transition area between IIIa and Iva
M.IIa-isllm3	muscle centre ventral lateral in transition area between IIa and IIIa	tergite of IIIa ventral lateral in transition area between IIIa and Iva
M.IIa-isllm4	muscle centre ventral lateral in transition area between IIa and IIIa	tergite of IIIa ventral lateral in transition area between IIIa and Iva
M.IIa-isllm5	muscle centre ventral lateral in transition area between IIa and IIIa	tergite of IIIa ventromedial in transition area between basal plate 1 and tergite IIIa
M.IIa-vtrm1	tergite of IIa ventre lateral	sternite of IIa medial
M.IIIa-llm1	muscle centrecentrallateral in transition area of IIa and IIIa	muscle centrecentrallateral IIIa
M.IIIa-llm2	muscle centrecentrallateral in transition area of IIa and IIIa	muscle centrecentrallateral IIIa

Name of the muscle	origin	insertion point
M.IIIa-llm3	muscle centrecentrallateral in transition area of IIa and IIIa	muscle centrecentrallateral IIIa
M.IIIa-istm1	inner side of the sternite III	muscle center dorsolateral in transition area between IIIa and IVa
M.IIIa-dvm1	muscle centrecentrallateral IIIa	tergite of IIIa mediolateral
M.IIIa-dvm2	muscle centrecentrallateral IIIa	tergite of IIIa mediolateral
M.IIIa-dvm3	muscle centrecentrallateral IIIa	tergite of IIIa mediolateral
M.IIIa-dvm4	muscle centrecentrallateral IIIa	tergite of IIIa mediolateral
M.IIIa-trm1	muscle centrecentrallateral IIIa	linked to M.IIIa-ret
M.IIIa-trm2	muscle centrecentrallateral IIIa posterior	dorsallateral in transition area between IIIa and IVa
M.IIIa-trm3	muscle centrecentrallateral IIIa posterior	basal plate 1 mediolateral anterior
M.IIIa-isdlm1	tergite of IIIa, anterior dorsal medial	tergite of Va, anterior dorsal medial in transition area between IVa und Va
M.IIIa-isllm1	muscle centre lateral in transition area between IIa and IIIa	sternite of IVa posterolateral in BP3
M.IIIa-ret	retinaculum at lateral side of ramus	linked to M.IIIa-trm1
M.IIIa-llm1	tergite lateral in transition area between IIa und IIIa	tergite lateral in transition area between IIIa und IVa
M.IIIa-llm2	tergite lateral in transition area between IIa und IIIa	tergite lateral in transition area between IIIa und IVa
M.IIIa-llm3	tergite lateral in transition area between IIa und IIIa	tergite lateral in transition area between IIIa und IVa
M.IIIa-llm4	tergite lateral in transition area between IIa und IIIa	tergite lateral in transition area between IIIa und IVa
M.IIIa-dlm1	muscle centre dorsomedial in transition area between IIa and IIIa	muscle centre dorsomedial in transition area between IIIa and IVa
M.IIIa-dlm2	muscle centre dorsomedial in transition area between IIa and IIIa	muscle centre dorsomedial in transition area between IIIa and IVa

Name of the muscle	origin	insertion point
M.IIIa-ldvm1	BP1 median lateral point	tergite IIIa lateral (very long longitudinal point)
M.IIIa-ldvm2	BP1 lateral transition area between BP1 and tergite IIIa	tergite IIIa lateral (very long longitudinal point)
M.IIIa-te.ret	muscle centrecentrallateral IIIa	retinaculum at lateral side of ramus
M.IVa-dlm1	tergite of IVa anterior dorsal medially	tergite of Va anterior dorsal medial
M.IVa-dlm2	tergite of IVa anterior dorsal medially	tergite of Va anterior dorsal medial
M.IVa-dlm3	tergite of IVa anterior dorsal medially	tergite of Va anterior dorsal medial
M.IVa-dlm4	tergite of IVa anterior dorsal medially	tergite of Va anterior dorsal medial
M.IVa-dlm5	tergite of IVa anterior dorsal medially	tergite of Va anterior dorsal medial
M.IVa-llm1	tergite of IVa anterior dorsal medially	ventrally in between the sternites BP1 and BP2
M.IVa-llm2	tergite of IVa anterior dorsal laterally	ventrally in between the sternites BP1 and BP2
M.IVa-dvm1	in the BP1, laterally in the basal rod	in the middle of IVa, laterally
M.IVa-isdlm1	tergite of IVa anterior dorsal medially	tergite of Va posteriorly in the BP3
M.IVa-isdlm2	tergite of IVa anterior dorsal medially	tergite of Va posteriorly in the BP3
M.IVa-isdlm3	tergite of IVa anterior dorsal medially	tergite of Va posteriorly in the BP3
M.IVa-isllm1	in the middle of IVa, lateral medially	tergite of Va posteriorly in the BP3
M.IVa-isllm2	in the middle of IVa, lateral medially	tergite of Va posteriorly in the BP3
M.Va-trm1	tergite of Va anterior dorsal medially	dorsal anteriorly at the BP3
M.Va-dlm1	tergite of Va anterior dorsal medially	tergite of VIa anterior dorsal medial

Name of the muscle	origin	insertion point
M.Man-dvm1	ventral medially at the anterior portion of the manubrium	dorsal medially at the anterior portion of the manubrium
M.Man-dvm2	ventral medially at the middle portion of the manubrium	dorsal medially at the middle portion of the manubrium
M.Man-lm1	basal plate 3 posterior dorsal medially	anterior laterally at the articulation point of manubrium

(please, insert the Table 1 here)

Basal plate 1 (BP1) and the basal rod (BR)

BP1 is the most prominent basal plate, originating from the inner posterior border of the 3rd abdominal segment, medially close to the retinaculum. Posteriorly it forms a border with BP2. BP1 has the most complex architecture. It is shaped like a swim float and has 2 walls, one on the inner side and another on the lateral border, allowing the board to assume a folded shape when seen in transversal or frontal perspective (Figs. 5A-F, 6A-B). The basal rod (BR) is the basal sclerite of BP1. It begins anteriorly, almost at the edge of the 3rd abdominal segment, on the side of the inner wall. The BR is initially narrow, assuming a thicker and flatter surface from the middle of BP1 up until the posterior end, where it connects to BP2 (Figs. 6A-B, 7A-K, 8A-B). At the posterior end of the basal rod are two finger-shaped depressions into which the basal condyle (bc) fits in the flexed furca state (Figs. 8C-E).

The muscles working anteriorly on BP1 and BR are M.IIIa-ldvm1 and M.IIIa-ldvm2, which connect the internal and external lateral wall of BP1, respectively with the lateral region of the 3rd abdominal segment. M.IIIa-istrm1, originating medially at the inner wall of BP1, connects anteriorly to the muscular center of the retinaculum, laterally to abdominal segments III and IV, as well as posteriorly to the lateral wall of BP1. In the middle of BP1, connected to the internal lateral wall, M.IVa-dvm1, the main dorsoventral muscle, can be found. This muscle is responsible for deforming BP1 and BR (Figs. 3A-B, 4, 8B, 9A-B).

Basal plate 2 (BP2) and basal sclerite 2 (BS2)

BP2 is triangular in shape and is positioned ventrolaterally, forming a corner between the abdomen and the furca. In the flexed furca state, this plate is telescoped internally. BS2 originates ventrally in BP2 (between BP1 and BP3) and extends vertically and laterally along the posterior edge of BP2, connecting to the ventral lateral edge of tergite V at the border between the abdomen and the furca (Figs. 5A-F, 7A-K, 8A-C, 10A-C)

Five muscles connect to BP2, two of them - M.IVa-llm1 and M.IVa-llm2 - to the anterior ventrolateral portion (on the border between BP1 and BP2). These two muscles run laterolongitudinally together,

assume a spiral shape, cross and support the muscle M.IVa-dvm1 and connect dorsally at the border between the 3rd and 4th abdominal segments. Laterally, on the dorsal surface at the corner of BP3, the muscles M.IVa-isdlm1, M.IVa-isdlm2 and M.IVa-isdlm3 connect (i.e. to the basal plate) (Figs. 3A-B, 4, 10A-E).

The Basal Plate 3 (BP3) and Basal Sclerite 3 (BS3)

At the base of the furca, is the basal plate 3 (BP3), the point of articulation between the basal sclerites BS2 and BS3. Here I recognize as BS3 the anterior part of the furca that articulates with the abdomen, and in flexion it pushes the basal sclerites to the center of the body. This sclerite connects to BP3 laterally and then extends ventrally in a V-shape (in transverse view) and merges in the midline. At the base of the BS3 there is a finger-shaped basal condyle that forms the point of contact between the furca and BR when the furca is flexed (Figs. 5A-F, 7A-K, 8A-C, 10A-E, 11A).

Two abdominal muscles connect to the dorsal lateral part of BP3, they are: M.IVa-isllm1, M.IVa-isllm2, both originate laterally, in the tergite of the 4th abdominal segment. M.IIIa-isllm1, starts dorsolaterally in the 3rd abdominal segment and extends posteriorly to connect at the base of the furca, in the BS3 (Figs. 3A-B, 4, 10A-E). Medially at the BP3 originate the M.Man-lm1, which connect posteriorly at the base of the posterior manubrium membrane (pmm) (Figs. 3A-B, 11A-E).

The furca: manubrium and dens

The furca connects ventrally to the 4th abdominal segment through BP3 and BS3, and when flexed it extends anteriorly along the midline to the first abdominal segment. This medial appendix is made up of 2 main parts, anteriorly the manubrium and posteriorly, the dens (Figs. 2A-C, 5A-B, 10A-E, 11A-J). With a tubular shape the manubrium is fused medially, and in the posterior portion there are two structures, dorsally a T-shaped furcular sclerite of the manubrium (fms), and ventrally a flexible membrane (pmm), both elastic structures border the dens. Anteriorly the dens is formed by two pads that together form the dens lock (dl), and then bifurcate posteriorly and with a series of crenulations assume the shape of a circular spring. These structures have internal channels through which the hemolymph flows between furca and abdomen, in both directions. Internally the dens pad, there is a transverse membrane of dens (dm). At the base of the dens, internally between each of its parts, there is a series of locks, where the retinaculum connects when the furca is flexed (Figs. 11A-E).

There are three pairs of muscles in the furca, present exclusively in the manubrium. M.Man-lm1 is a longitudinal muscle that originates medially in the anterior portion of BP3 and connects posteriorly on the lateral side of the manubrium, right at the base of pmm, the articulation point with the dens. The other two pairs are dorsoventral. M.Man-dvm1 is present anteriorly, and M.Man-dvm2 solely in the middle portion of the manubrium (Figs. 3A-B, 11A-E).

The retinaculum

Ventromedially in the posterior portion of the 3rd abdominal segment, the retinaculum is situated. This very small and unremarkable structure has an elastic cuticular composition that permits deformation, and an architecture capable of holding the furca at rest. It is a triangular-shaped structure with 2 arms at its end (the rami), each one with 4 teeth. Internally at the base of each of the rami, a pivot point is located (Figs. 2A-C, 12A-E).

Internally a complex muscular system supports the inherent movements of this structure. Connecting internally to the retinaculum in the region of the point of articulation are the short muscles M.IIIa-ret. At the base of this, a connection point with M.IIIa-trm1 and the M.IIIa-te.ret tendon can be found. Both these muscles connect internally to a complex muscle center composed of M.IIIa-trm2, M.IIIa-istrm1 and M.IIIa-istm1 (Figs. 3A-B, 4, 12A-E, 13A-D).

Morphofunctional aspects related to jumping

Spring mechanism, triggers and energy storage

The cLSM and MicroCT images revealed the areas of the jump apparatus that are most elastic and have energy storage potential. The spring mechanism is generated in BP1, BP2, BP3, mainly from the deformation of their respective basal sclerites. Such deformation and energy storage is made possible by the elasticity of these structures, which are rich in resilin. The tension in the sclerites is generated by muscular action, hydrostatic pressure and in large part by tension between the furca and the basal sclerites when furca is flexed. Four main kinematic zones can be identified in the furca: BS3 right at the base of the manubrium, which extending posteriorly connects the furcular area of the manubrium zone (FMZ) with strong posterior sclerite (fms), and laterally the posterolateral manubrial zone (PLMZ) where a flexible membrane (pmm) is present. Both posterior manubrial zones, articulate with the anterior zone of dens (ADZ), the main point of contact between the furca and the surface (Figs. 7A-K, 8A-C, 11A-H).

The spring mechanism is intensified by the presence of the trigger, the retinaculum, which increase the tension between the basal plates and prevents the basal sclerites from returning to a relaxed state. At the base of the furca a basal condyle (bc) at BS3 intensifies the tension on the basal sclerites and extends posteriorly along with the manubrium as a keel, coming into direct contact with the ventral part of the abdomen when the furca is flexed (Figs. 8D-E, 10A-E, 12A-G, 13C-D).

Hydrostatic pressure

Hydrostatic pressure plays a passive role in jumping by increasing the tension of the basal plates, and an active role by increasing the efficiency of the jump in coordination with the muscles. Thereby the hemolymph is concentrated inside the body cavity, tensing its walls in a dorso-ventral and longitudinal movement when the furca is flexed. With the release of the furca, this hydrostatic volume is directed ventrally and posteriorly toward the furcular cavity (Fig. 11A-E).

In the abdomen, the muscles related to the increase in hemolymphatic pressure are mainly the dorso-longitudinal muscles (M.IIa-isdlm1, M.IIa-isdlm1, and the dlm), dorsoventral (M.IVa-dvm1), ventral and

lateral longitudinal muscles. The contraction of these muscles causes a reduction in the space between the segments and, consequently, an increase in hydrostatic pressure. At the moment of extension, M.IIIa-istm1 may have an important role in directing pressure to the basal plates by deforming the 3rd abdominal segment dorsoventrally and decreasing the opening for hydrostatic flow to the posterior abdominal region. The pleural muscles M.IIIa-istrm1, M.IIIa-ldvm1 and M.IIIa-ldvm2 and the ventral longitudinal lateral intersegmental muscles MIIa-isllm1, MIIa-isllm2, MIIa-isllm3, MIIa-isllm4 and M.IIa-isllm5 could act by regulating the hydrostatic pressure between the lateral tergites (IIIa-IVa), sternite III and BP1 in the anteroposterior flow towards the opening cavity of the furca (Figs. 3A-B, 4, 8A-E, 9A-B, 10A-E, 14A-B).

In the furca, the dorsoventral (M.Man-dvm1, M.Man-dvm2) and longitudinal muscles (M.Man-lm1) are involved in controlling hemolymphatic pressure by compressing the cuticle walls, effectively injecting hemolymph into the dens cavity. As already mentioned, the muscles (M.Man-lm1) potentially also act by releasing the furca from the retinaculum (Figs. 11A-E, 14A-B).

Transition between "flexed furca" and "extended furca" phases

The flexed furca phase starts with the engagement of the retinaculum in the locks of the dens, with the help of muscles M.IIIa-trm1, M.IIIa-te.ret and M.IIIa-ret, which through their contraction set up the hook, when the furca returns to the ventral side of the abdomen (Figs. 12D-E). The return of the furca to the abdomen potentially occurs by the combined contraction of muscles M.IVa-dvm1 (which connects to BP1), M.IVa-ll1 and M.IVa-ll2 (which connect at the border between BP1 and BP2) and the long M.IIIa-isllm1 (which connects to BS3 at the base of the furca) (Figs. 10A-E, 14A-B). The furca extension phase begins with the release of the furca by the retinaculum when extension is needed. It has been proposed that the furca is released from the retinaculum by hydrostatic pressure alone (this will be addressed in the discussion section), but here I propose an alternative hypothesis. The contraction of the longitudinal manubrial muscle M.Man-lm1 through the articulation with the dens (which is almost like a knee), creates the pull on the posterior side of manubrium, the posterior manubrial membrane (pmm) and their sclerites. This causes an opening of the dens pads, resulting in the opening of the dens lock, and the release of the furca (Figs. 12F-G). Subsequently, the contraction of muscles M.IVa-isdlm1, M.IVa-isdlm2, M.IVa-isdlm3, M.IVa-isllm1 and M.IVa-isllm2 could extend the furca (Figs. 10A-E, 14A-B, 15A-B) and, together with the spring and the hemolymphatic mechanisms (or even without, but with loss of efficiency), result in jumping.

Discussion

It has been suggested (Christian, 1979; Brackenbury & Hunt, 1993; Sudo et al, 2013a and b) that the strategies and mechanisms involved in jumping vary between species that have distinct segmentation and are cylindrical in shape (such as *Orchesella cincta* and *Tomocerus* spp.), and those with fused segmentation which are globular in shape (such as *Sminthurus* spp.). However, all taxa (except for those with secondary loss of the furca and retinaculum) essentially and primarily use the furca as a catapult

and the retinaculum as a trigger (Manton, 1972; Eisenbeis & Ulmer, 1978; Christian, 1979; Brackenbury & Hunt, 1993). Favret *et al.*(2015) additionally suggested that the ventral tube, when adhered to the substrate, could serve to act on the direction and trajectory of the jump, but this is not something evaluated in this study.

Several studies (Manton, 1972; Eisenbeis & Ulmer, 1978; Christian, 1979; and Brackenbury & Hunt, 1993) agree that the basal plates play an important role in creating the spring mechanism. Manton (1972) and Christian (1979) recognized the basal rods as the structures in which elastic energy is stored. Eisenbeis & Ulmer (1978) and Brackenbury & Hunt (1993) suggested that this energy is stored not only in the basal rods, but also in other basal sclerites (such as BS2 and BS3). Eisenbeis & Ulmer (1978) were the first to suggest that elastic energy could be stored by the resilin present in the cuticle of the basal plates and especially in the basal sclerites of springtails. Gronemberg (1996) declared the energy storage mechanism in springtails as occurring through the cuticle, without mentioning the resilin or the basal sclerites. According to Sudo et al. (2013b), the elastic energy produced is stored in the muscles and subsequently released as kinetic energy, but there is no mention of which muscles specifically. I agree with the idea that energy is stored in BP1, BP2 and BP3 and their respective sclerites (BR, BS2 and BS3), and also in the kinematic zones demarcated in the furca (Figs. 11F-H). Evidence for this can be found in the cLSM images provided by this study, which at a wavelength of 405nm reveal the presence of resilin in these structures, corroborating Burrows et al. (2008) and Büsse & Gorb (2008).

There is a converging opinion, and I share it, that hydraulic pressure acts on the efficiency of the jump (Noble-Nesbitt, 1963; Manton 1972; Christian, 1979; Eisenbeis & Ulmer, 1978; Brackenbury & Hunt, 1993). Manton (1972) actually hypothesized that furca extension and jumping are not brought about directly by muscle force, but predominantly by hydraulic pressure. However, this was disputed by Christian (1979) and Eisenbeis & Ulmer (1978) (and also this study), who put forward the hypothesis that furca extension is primarily the result of muscular force, independent of hydrostatic pressure. On the other hand, Brackenbury & Hunt (1993) rejected the idea of furca extension being brought about predominantly by muscular action, describing the muscles attached to the manubrium as having a very weak line of action and a small total mass. In my opinion, muscular force would be sufficient to open the furca and even to permit jumping, but would be incomparably less effective alone than when combined with hydrostatic force. Eisenbeis & Ulmer (1978) show and describe possible channels through which hemolymph flows. Cylindrical and segmented species like *O. cincta* possess the ability to telescope the abdominal segments and the tergo-pleural arches (Manton 1972; Christian 1979), primarily by using of the dorsal and lateral longitudinal muscles of the trunk (Manton 1972). This phenomenon has been suggested to be the main mechanism behind hydraulic pressure (Manton 1972; Brackenbury & Hunt 1993), and by my observations support this hypothesis.

It is widely accepted that the retinaculum acts as a trigger, and by holding the furca permits the creation of the spring mechanism (Christian, 1979; Brackenbury & Hunt, 1993; Sudo et al. 2013a and 2013b; Manton, 1972; Eisenbeis & Ulmer, 1978). According to Manton (1972), the distension of the retinaculum is the result of the hydrostatic pressure generated by the trunk muscles, while its retraction is mediated by

the action of the muscles directly connected to it (M.IIIa-ret). However, it is still not clear how the retinaculum could be selectively everted - in other words why such hydraulic pressure does not act at the same time, for example, in the eversion of the ventral tube. Manton (1972) suggested that the pleural muscles M.IIIa-trm3, M.IIIa-ldvm1 and M.IIIa-ldvm2 may be directly involved in bracing the flexible basal parts of the body wall against increased hydrostatic pressure and thus strengthening the action of the longitudinal sternal muscles (M.IIa-isllm3, M.IIa-isllm4 and M.IIa-isllm5) in the vicinity of the retinaculum. My observations make it seem much more likely that hydrostatic pressure is not necessary for the release of the furca by the retinaculum, and that this occurs by the exclusive force of one muscle, M.Man-lm1.

Despite the differences in the jumping mechanisms among Collembola species, jumping in all of them features the following phases : 1) the take-off phase, between the start of furca movement and the moment the animal stops touching the ground; 2) the aerial phase, which ends when the animal touches the ground again; and 3) the landing phase, when the animal touches the ground for the first time after the jump (Sudo *et al.*2013b; Christian 1979). Christian (1979) described jumping in *O. cincta* as involving similar movements to jumping in *Heteromurus nitidus* (Templeton, 1835), a closely phylogenetically related Entomobryid, though *O. cincta* did not jump as far or as high. Jumping in *O. cincta* starts with a change in the longitudinal axis of the body. The animal bends, bringing head, legs and furca toward the ground. With the release of the furca, there is a projection of the body backward. The body acquires angular impulse, then moves over the dens until the animal is standing up straight and aligned with the longitudinal axis of the body. The weight and force of the body is then transferred to the distal part of the dens and the substrate surface, which relieves tension in the manubrium-dens joint and confers stability to the movement. For the extension of the furca the body assumes a curved concave dorsal contour, probably due to the contraction of direct and indirect extensor muscles (Christian 1979). Eisenbeis & Ulmer (1978) recognize as extensors of the furca the muscles M.IVa-isdlm1, M.IVa-isdlm2 and M.IVa-isdlm3, together with the longitudinal muscles and the intersegmental M.IIIa-isllm1. According to them, the extensor traction acts first on the medial and lateral parts of BP3 and BS3, and is then transferred to the manubrium, with opening aided by increased hemolymphatic pressure. Finally the manubrial muscles M.Man-dvm1, M.Man-dvm2 and M.Man-lm1 expand and spread the dens and compress the manubrium (Eisenbeis & Ulmer, 1978). In Christian's (1979) experiments, *O. cincta* had a maximum extension speed equivalent to 290 rad s-1, which indicates how quickly the manubrium is unfolded in this species. The angle of body rotation at take-off was 71°, with a rotation speed of 102 rad s^{-1} after the take-off phase. The animals achieved a height of 6mm during the jump. Apparently, all springtails exhibit a backward rotation, as shown by Christian (1979) and Sudo *et al.*(2013a and 2013b). Brackenbury & Hunt (1993) hypothesized that this is explained by the position and length of the the furca, which ends below or in front of the body's center of mass. The release of the furca thus causes an imbalance to this center, and the furca creates a backward rotation. Brackenbury & Hunt (1993) and Sudo *et al.*(2013a) agree that spinning while jumping could be a waste of energy, but Sudo *et al.*(2013a) also suggest that it may be a mechanism by which springtails control the height and direction of their jump. This challenges Christian (1979), who suggested that the direction of the jump and the landing site are possibly random.

Conclusions

Jumping in springtails involves mechanisms and a morphological apparatus unique to this group of arthropods. By studying the morphology of a springtail and comparing the "furca flexed" and "furca extended" phases, we were able to gain a deeper understanding of the mechanisms involved in jumping. Springtails with distinct segmentation possibly have mechanisms for hydrostatic regulation which are distinct [i.e. different] from those with fused segmentation. Energy appears to be stored in resilin elastic cuticular structures. A detailed morphological study revealed interesting cuticular characters such as basal plates and sclerites. The present study provides useful information for future phylogenetic and morphofunctional studies. To gain a better insight into the precise movements involved in the different phases of jumping, an analysis of video and image records made using a high speed camera would be helpful.

Methods

Specimens sampling and fixation

The morphology of the jumping apparatus was studied comparatively between 10 specimens of *Orchesella cincta* with extended (T101-T110) and 6 specimens with flexed furca (T201-T206) (Figs. 2A-C). Abdominal segments 2–6 were reconstructed, including cuticular structures such as basal plates and sclerites, as well as internal musculature. The animals were found in the garden of the Institute of Zoology at the Universität Rostock, in the surface layer of leaf litter, using an entomological aspirator. The specimens were immersed in two fixatives depending on the microscopy procedure, Duboscq-Brasil fixative for study using Micro Computer Tomography (MicroCT), and PFA fixative (4% in PBS) for study using Confocal Laser Scanning Microscopy (cLSM). Voucher specimens are deposited at the Institute of Zoology at the Universität Rostock.

Confocal Laser Scanning Microscopy (cLSM) - PFA (4% in PBS)

Here, two approaches were taken: 1) to investigate the cuticular elastic structures, specimens were not stained and were exposed to a wavelength of 405 nm; 2) to investigate muscular tissues, specimens were stained with Phalloidin staining and exposed to a wavelength of 555 nm. For both approaches the specimens were transferred alive and immersed in PFA solution (4% in PBS) for at least 1h. Subsequently, the specimens were washed in PBS (1x Phosphate-Buffered Saline) solution in 3 steps of 5 min each, then washed in 0.05 NaN_3 PBS (Natrium-Azid) solution for 5 min, and finally transferred to the refrigerator.

The specimens for Phalloidin staining were then subjected to another chemical treatment series. First, they were washed in PBT (PBS + Triton X-100) in 4 steps of 25 min, then, in a light-protected environment, immersed in 1 µl of phalloidin and 1 ml of PBT solution for 90 min. Subsequently they were immersed in 3 PBS baths, the first for 3 min, and the last two for 15 min, and then transferred to 1x PBS + 0.05% NaN_3. Finally, they were transferred to 1x PBS + 0.05% NaN3 and refrigerated at 5°C.

The specimens were mounted between two glass coverslips (60mm x 24mm), then immersed in 100% glycerin or in RapiClear 1.47, SunJin Lab (when heavily pigmented). Modeling clay was used to seal the four edges. Slides were then taken to the cLSM (LEICA Stellaris 8) and studied at 405 nm (without staining) and 555 nm (with Phalloidin staining). The slides were kept in the dark and refrigerated (5°C) when not in use.

Micro Computer Tomography (MicroCT)

The specimens were fixed for at least 1h in Duboscq-Brasil then washed to dehydrate them in a series of different concentrations of alcohol (ethanol) starting at 20% and proceeding up to 99.8% (20%, 30%, 40%, 50%, 60%, 70%, 80%, 90% and 98.8%) (each step 10 min). They were later transferred to the Leica EMCPD300 equipment for critical point drying, then mounted with white liquid glue on toothpicks for study under Micro Computer Tomography (ZEISS Xradia 410 Versa X-Ray).

Scanning Electron Microscopy (SEM)

The specimens were initially transferred to 20% ethanol and then subjected to a series of dehydrating solutions (20%, 30%, 40%, 50%, 60%, 70%, 80%, 90% and 98.8%) (each step 10 min) and critical point dried using the Leica EMCPD300 equipment. Subsequently, they were prepared on metallic pins to be sputter-coated with gold using a Sputter Coater EM SCD 004.

3D Reconstruction

Stacks of digital images obtained using MicroCT or cLSM were processed using the 3D reconstruction software Amira 2020.2. Data processing primarily involved segmentation of structures of interest - that is, the marking of specific structures at regular intervals within the image stack. On the basis of the segmentation, the software is able to create a surface rendering representing a 3D reconstruction of the morphological structure in question.

Terminology

The abdominal segments studied are II, III, IV, V, and VI. The terminology for the following abdominal structures is adopted from Eisenbeis & Ulmer (1978): BP1 - basal plate 1, BP2 - Basal plate 2, BP3 - Basal plate 3, BR - Basal Rods. Retinaculum and furca are described from Schaller (1970): Rt - retinaculum, Ct - retinaculum körper (corpus tenaculi), R - retinaculum ramus, F - furca, M - manubrium, D - dens. I rename the basal sclerites of basal plates 2 and 3, as BS2 (Basal sclerite 2) and BS3 (Basal sclerite 3), respectively.

The terminology for the name of the abdominal muscles is based on the following system. The names consist of three sections: Example: M.IVa-isllm1. The prefix indicates the type of structure and its previous point of origin. The prefix takes the capital letter representing the type of structure, M in this example means a muscle. Endosclerites with an E, and tendon names would begin with a T, etc. The roman numeral e in sequence represents the segment in which such a structure (M, E or T) originates,

previously. The lowercase letter directly linked to the Roman numeral indicates whether the segment is cephalic (c), thoracic (t), or abdominal (a). The stem is separated from the suffix by a hyphen. The suffix consists of an abbreviation and an Arabic numeral. The abbreviation represents the orientation and position of the muscles in the body.

Abbreviations

DLM	dorsal longitudinal muscles
DLLM	dorsolateral longitudinal Muscles
DVM	dorsoventral muscles
ISDLM	intersegmental dorsolongitudinal muscles
ISDVM	intersegmental dorsoventral muscles
ISLM	intersegmental longitudinal muscles
ISLLM	intersegmental laterolongitudinal muscles
LDVM	lateral dorsoventral muscles
LLM	lateral longitudinal muscles
BP1	basal plate 1
BR	basal rod
BP2	basal plate 2
BP3	basal plate 3
BS2	basal sclerite 2
BS3	basal sclerite 3
CT	corpus tenaculi
RT	retinaculum
D	dens
M	manubrium
F	furca
R	retinaculum ramus
PMM	posterior manubrium membrane
BC	basal condyle
DM	dens membrane
FMS	furcular sclerite of the manubrium
DL	dens lock
cLSM	confocal laser scanning microscopy
3D	third dimension
MicroCT	micro computer tomography

SEM	scanning electron microscopy
PFA	paraformaldehyde
PBS	1x phosphate-buffered saline
PBT	PBS + Triton X-100
NaN_3	sodium azide

Declarations

Ethics approval and consent to participate

Not applicable

Consent for publication

Not applicable

Availability of data and materials

The datasets used and/or analysed during the current study are available from the corresponding author on reasonable request.

Competing interests

The authors declare that they have no competing interests

Funding

Deutsche Forschungsgemeinschaft (DFG) – Projektnummer 442589507

Authors contributions

Not applicable

Acknowledgements

I am grateful to Stephan Scholz for carrying out the scans. I also thanks to Kerstin Schwandt for all the support in the lab. I also thank the colleagues M.Sc. Alice Günther, Birk Rillich, Dr. Diego S. Porto and Prof. Dr. Stefan Richter for valuable contributions. I also acknowledge Lucy Cathrow for improving the English. The cLSM and the MicroCT machine at Universität Rostock were jointly sponsored by the Deutsche Forschungsgemeinschaft (DFG INST 264/185 FUGG and DFG INST 264/130-1 FUGG, respectively) and the Land Mecklenburg-Vorpommern.

References

1. Agolin M, D'Haese CA. An application of dynamic homology to morphological characters: Direct optimization of setae sequences and phylogeny of the family Odontellidae (Poduromorpha, Collembola). Cladistics. 2009;25(4):353–85. DOI:10.1111/j.1096-0031.2009.00272.x.
2. Brackenbury J, Hunt H. Jumping in springtails: mechanism and dynamics. J Zool. 1993;229:217–36. https://doi.org/10.1111/j.1469-7998.1993.tb02632.x.
3. Bretfeld G. Zur Anatomie und Embryologie der Rumpfmuskulatur und der abdominalen Anhänge der Collembolen. Zool Jb. 1963;80:76.
4. Burrows M, Shaw SR, Sutton GP. Resilin and chitinous cuticle form a composite structure for energy storage in jumping by frog hopper insects. BMC Biol. 2008;6:41. https://doi.org/10.1186/1741-7007-6-41.
5. Büsse S, Gorb SN. Material composition of the mouthpart cuticle in a damselfly larva (Insecta: Odonata) and its biomechanical significance. Royal Soc Open Sci. 2018;5:172117. http://dx.doi.org/10.1098/rsos.172117.
6. Christian E. The Jump of the Springtails. Naturwissenschaften. 1979;6:495–6 pp. DOI:10.1007/BF00702849.
7. Eisenbeis G, Wichard W. Atlas in the Biology of soil. XIV, 437; https://doi.org/10.1007/978-3-642-72634-7.
8. Eisenbeis G. Die Thorakal- und Abdominal-Muskulatur von Arten der Springschwanz-Gattung Tomocerus (Collembola: Tomoceridae). Entomologica Germanica. 1978;4(1):55–83.
9. Eisenbeis G, Ulmer S. Zur Funktionsmorphologie des Sprung-Apparates der Springschwanze am Beispiel von Arten der Gattung Tomocerus (Collembola: Tomoceridae). Entomol Generalis. 1978;5:35–55. DOI:10.1127/entom.gen/5/1978/35.
10. Favret C, Tzaud M, Erbe EF, Bauchan GR, Ochoa R. An Adhesive Collophore May Help Direct the Springtail Jump. Ann Entomol Soc Am 2016; 1–6; https://doi.org/10.1093/aesa/sav078.
11. Gisin H. Ökologie und Lebensgemeinschaften der Collembolen im schweizerischen Excursionsgebiet Basels. Revue Suisse de Zoologie. 1943; 50 pp.
12. Gronenberg W. The fast mandible strike in the trap-jaw ant *Odontomachus*: temporal properties and morphological characteristics. J Comp Physiol A. 1969;176:391–8.
13. Gronemberg W. Fast actions in small animals: springs and click mechanisms. J Comp Physiol A. 1996;178:727–34.
14. Haug JT, Haug C, Kutschera V, Mayer G, Maas A, Liebau S, Castellani C, Wolfram U, Clarkson E, Waloszek D. Autofluorescence imaging, an excellent tool for comparative morphology. J Microsc. 2011;244:3. https://doi.org/10.1111/j.1365-2818.2011.03534.x.
15. Hopkin SP. Biology of the Springtails (Insecta: Collembola). Oxford University Press; 1997.
16. Ilton M, Bhamla MS, Ma X, Cox SM, Fitchett LL, Kim Y, Koh JS, Krishnamurthy D, Kuo CY, Temel FZ, Crosby AJ, Prakash M, Sutton GP, Wood RJ, Azizi E, Bergbreiter S, Patek SN. The principles of

cascading power limits in small, fast biological and engineered systems. Science. 2018;360:eaao1082. DOI:10.1126/science.aao1082.

17. Konopova B, Akam M. The Hox genes Ultrabithorax and abdominal-A specify three different types of abdominal appendage in the springtail *Orchesella cincta* (Collembola). EvoDevo. 2014;5:2. https://doi.org/10.1186/2041-9139-5-2.
18. Manton SM. The Arthropoda: Habits, Functional Morphology and Evolution. Oxford University Press; 1972.
19. Noble-Nesbitt J. A site of water and ionic exchange with the medium in *Podura aquatica* L. (Collembola, Isotomidae). J. exp. Biol. 1963; 40,701 – 71 1.
20. Palacios-Vargas JG, Mejía-Recamier BE. Técnicas de colecta. In: t*écnicas de colecta, preservación y montaje de microartrópodos*. Las Prensas de Ciencias, UNAM; 2007. pp. 23–46.
21. Panina IV, Potapov MB, Polilov AA. Effects of miniaturization in the anatomy of the minute springtail Mesaphorura sylvatica (Hexapoda: Collembola: Tullbergiidae). PeerJ. 2019; 1–28. DOI:10.7717/peerj.8037.
22. Rusek J. Biodiversity of Collembola and their functional role in the ecosystem. Biodivers Conserv. 1998;7:1207–19pp.
23. Schaller F Collembola (Springschwänze). Handbuch der Zoologie. 1970; Bd. 4, pp. 72.
24. Sudo S, Shiono M, Kainuma T, Shirai A, Hayase T. Observations on the springtail jumping organ and jumping mechanism worked by a spring. J Aero Aqua Bio-mechanisms. 2013a;3:1. DOI:10.5226/JABMECH.3.92.
25. Sudo S, Shiono M, Kainuma T, Shirai A, Hayase T. The kinematics of jumping of globular springtail. J aero aqua bio-mechanisms. 2013b;3:1. https://doi.org/10.5226/jabmech.3.85.
26. Whalley P, Jarzembowski EA. A new assessment of Rhyniella, the earliest known insect, from the Devonian of Rhynie, Scotland. Nature. 1981;291:317. https://doi.org/10.1038/291317a0.

Figures

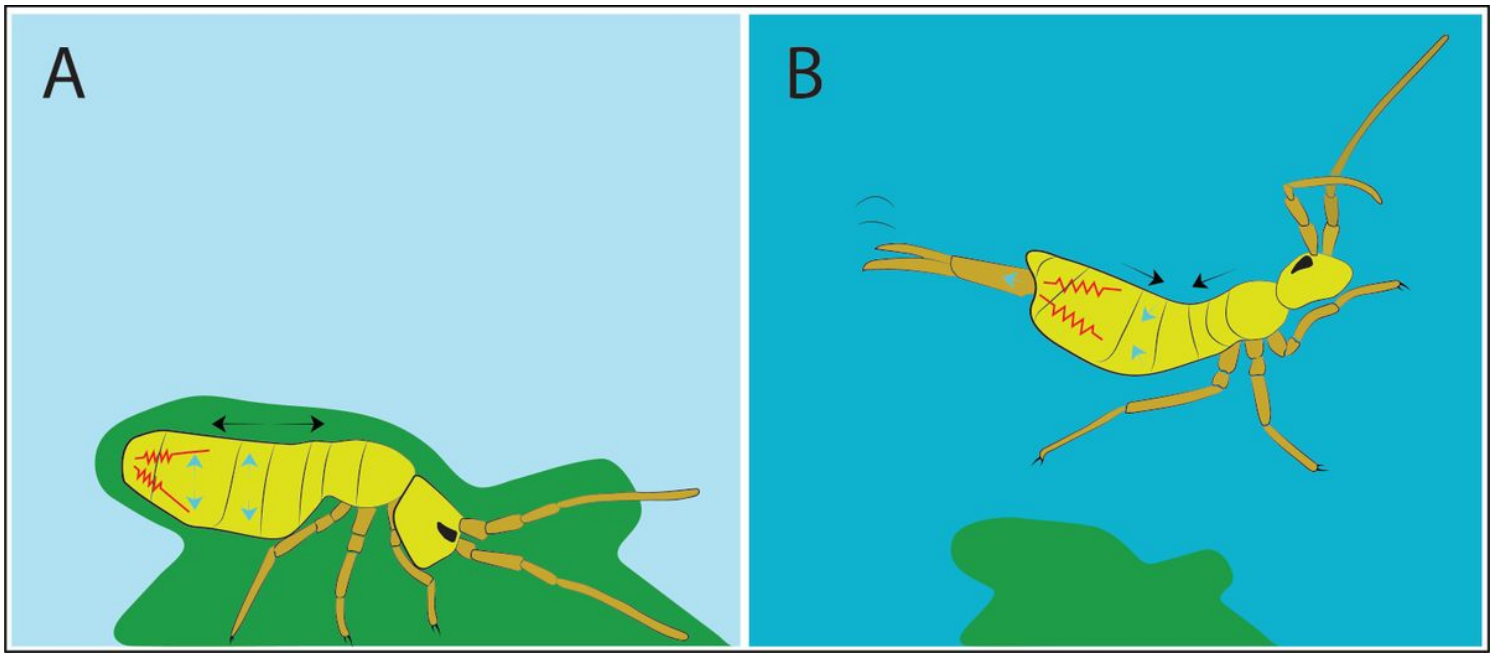

Figure 1

Schematic image of springtails jumping. A) Furca flexed at rest, spring contracted, B) Furca extended during jump, spring relaxed. Black arrows show the contour of the segments. Blue arrows show hydrostatic flow. Red springs show the spring mechanism.

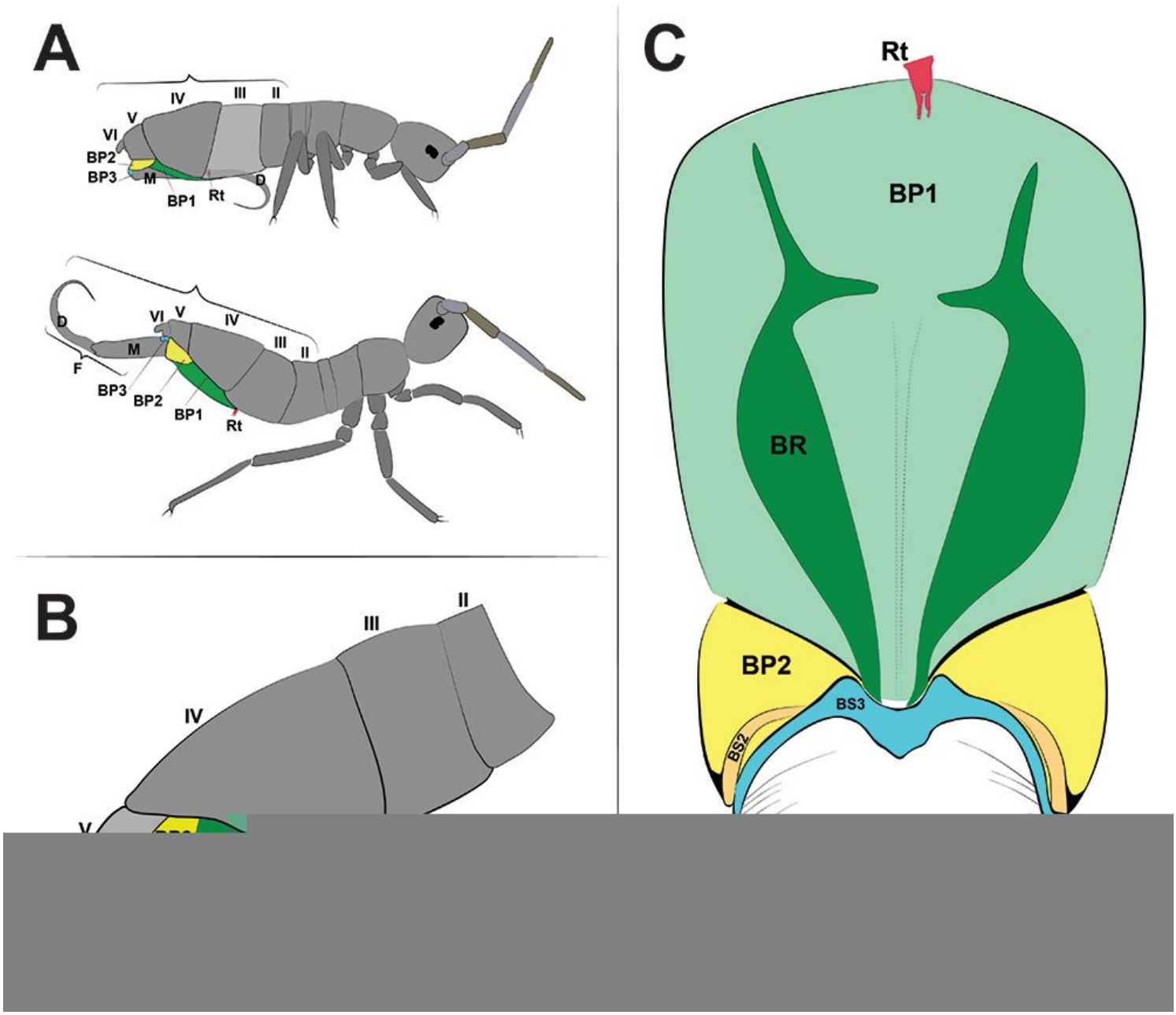

Figure 2

Morphofunctional study of the jumping apparatus in *Orchesella cincta*. A) The reconstructed abdominal segments and a comparison between flexed and extended furca phases. B) Lateral view of the jumping apparatus, comprised of abdominal segments 2-6. C) Ventral view of the jumping apparatus - adapted from Manton (1972) on *Tomocerus longicornis* (Müller, 1776). BP1: Basal plate 1, BP2: Basal plate 2, BP3: Basal plate 3, M: Manubrium, F: Furca, D: Dens, R: Retinaculum, BR: Basal rods, BS2: Basal sclerite 2, BS3: Basal sclerite 3.

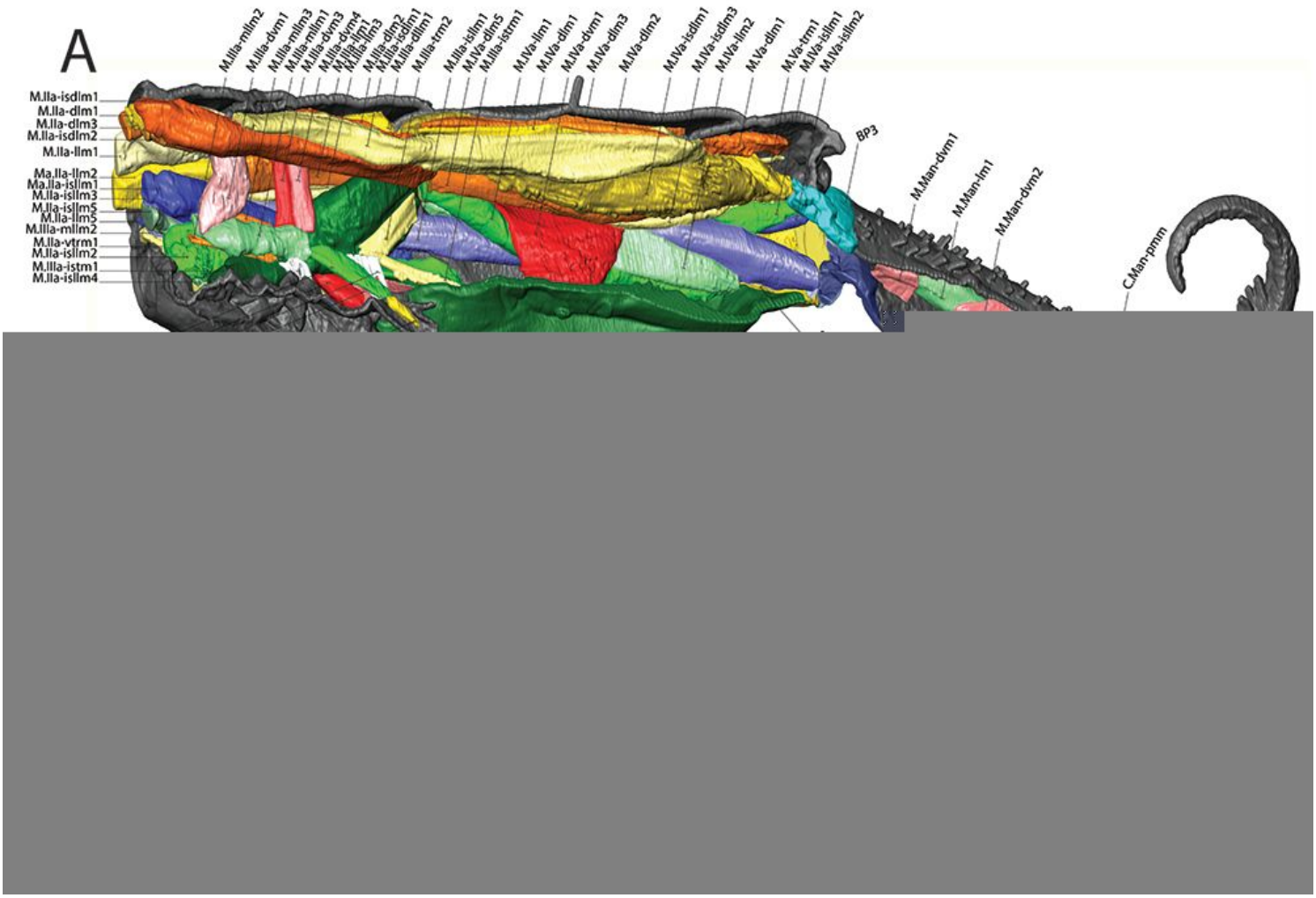

Figure 3

MicroCT morphological reconstruction of the 2nd - 6thabdominal segments, the jumping apparatus, cuticle and musculature in *Orchesella cincta* with the furca extended. A) Internal lateral view of the jumping apparatus (furca extended). B) External lateral view of the jumping apparatus (furca extended).

Figure 4

MicroCT morphological reconstruction of the 2nd - 6th abdominal segments, the jumping apparatus, cuticle and musculature in *Orchesella cincta* with the furca flexed. Internal lateral view of the jumping apparatus (furca flexed).

Figure 5

MicroCT morphological reconstruction of the Basal plates of *Orchesella cincta*. A) Lateral view of the jumping apparatus (extended). B) Ventral view of the jumping apparatus (flexed). Sternites and basal plates. C, E) Furca extended. D) Furca flexed in dorsal view. F) Furca flexed in ventral view (furca removed). F) BP1: basal plate 1, BP2: basal plate 2, BP3: basal plate 3, M: manubrium, D: dens, R: retinaculum, BR: basal rods.

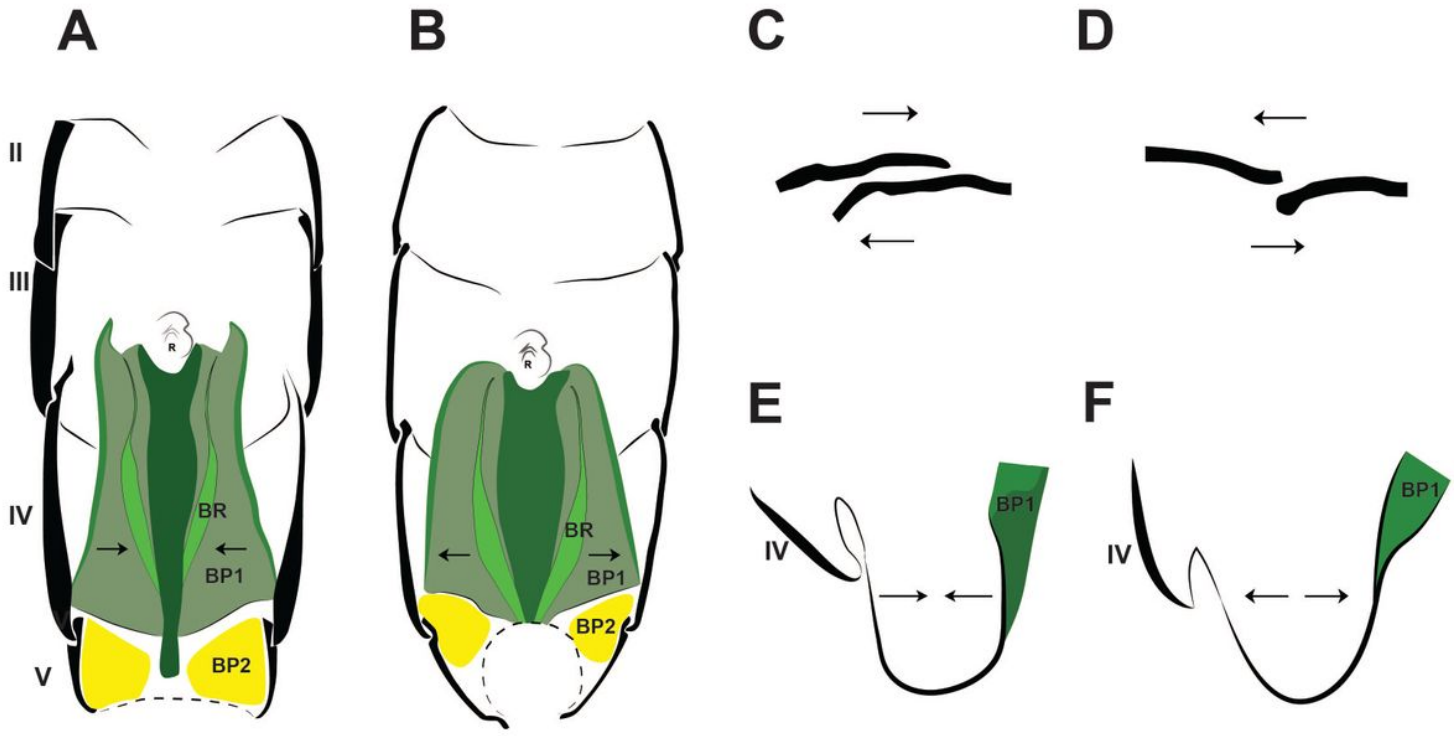

Figure 6

Schematic image of the functioning of cuticular structures such as tergites, sternites, basal plates, and sclerites during jumping behavior in *Orchesella cincta*. A) Furca extended. B) Furca flexed. C) Tergites of the 3rd and 4th abdominal segments (furca extended). D) Tergites of the 3rd and 4th abdominal segments (furca flexed). E) Transversal view of basal plate 1 (Furca extended). F) Transversal view of basal plate 1 (furca flexed). BP1: basal plate 1, BP2: basal plate 2, R: retinaculum, BR: basal rods.

Figure 7

Comparative view of the basal sclerites when furca flexed and furca extended in *Orchesella cincta*. A) Lateral view of the jumping apparatus (furca extended). B) Lateral view of the jumping apparatus (furca flexed). C) Ventral view of the jumping apparatus (furca extended). D-K) Basal sclerites (cuticle

transparency). D) Posterior view (furca extended). E) Posterior view (furca flexed). F) Dorsal view (furca extended). G) Dorsal view (furca flexed). H) Lateral view (furca extended). I) Lateral view (furca flexed). J) Ventral view (furca extended). K) Ventral view (furca flexed).

Figure 8

cLSM images showing the muscles which connect to BP1, the sclerites with which the furca articulates with the abdomen and the basal condyle in *Orchesella cincta*. A) The basal sclerites at 405 nm. B) The basal sclerites at 555 nm (stained with phalloidin). C) The basal sclerites at 405 nm. D) Schematic images of the functioning of the abdominal basal sclerites in the extended and flexed furca states.BR: basal rods, BS2: basal sclerites 2, BS3: basal sclerites 3, BC: basal condyle.

Figure 9

The musculature connected to BP1 in *Orchesella cincta*. Muscles M.IVa-dvm1, M.IIIa-ldvm1, M.IIIa-ldvm2 and M.IIIa-istrm1 (3D reconstruction of IIa-IVa, seen from dorsal without tergites. A) Muscles M.IVa-dvm1, M.IIIa-ldvm1, M.IIIa-ldvm2 and M.IIIa-istrm1. B) Comparative schematic view of the functioning of the muscles connected to BP1 with furca extended and flexed. 1) Posterior region of the 4^{th} abdominal segment. 2) Middle of the 4^{th} abdominal segment. 3) Anterior region of the 4^{th} abdominal segment. 4) Posterior region of the 3^{rd} abdominal segment. BP1: basal plate 1, BP2: basal plate 2, BR: basal rods.

Figure 10

Morphological reconstruction of the lateral side of the 4^{th}-6^{th} abdominal segments, BP1, BP2 and BP3 and basal sclerites in *Orchesella cincta* and the insertion points of the musculature. A) External lateral view of the posterior portion of the 4^{th} and 5-6^{th} abdominal segments. B) Internal lateral view of the posterior portion of the 4^{th} and 5-6^{th} abdominal segments. C) Internal frontal view of BP2 and BP3. D-E) Schematic representation showing how basal plates BP1, BP2 and BP3 and the muscles function in the construction of the spring mechanism. D) Furca flexed. E) Furca extended. M: manubrium, D: dens, BR: basal rod, BC: basal condyle, BS2: basal sclerite 2, BS3: basal sclerite 3, BP3: basal plate 3, basal plate 1, BP2: basal plate 2, BR: basal rods.

Figure 11

Morphological reconstruction of the furca and kinematic zones. A) Structures of the furca, B) T-shaped furcular sclerite of the manubrium (fms), C) Dens lock, D) One side of the dens lock (seen from the inside), E) Schematic representation showing structures of the furca. F-H) Kinematic zones of the jumping mechanism. M: manubrium, D: dens, BR: basal rod, BS2: basal sclerite 2, BS3: basal sclerite 3, BP3: basal plate 3, basal plate 1, BP2: basal plate 2, BR: basal rods, fms: furcular manubrium sclerite, dm: membrane of dens, dl: dens lock, pmm: posterior membrane of manubrium, FMZ: furcular manubrial zone, PLMZ: posterolateral manubrial zone, ADZ: anterior zone of dens.

Figure 12

Morphology and function of the retinaculum. A) Scanning electron microscopy (SEM) image (anterior view) of the retinaculum, B) Confocal microscopy (cLSM) image at 405 nm (view from anterior) of the retinaculum, C) Confocal microscopy (cLSM) image at 555 nm (stained with phalloidin) (view from anterior) of the retinaculum, D) Morphological reconstruction using micro computer tomography (MicroCT) (view from posterior) of the retinaculum, E) Schematic representation showing the muscular function of the retinaculum, F-G) Schematic representation showing a hypothesis on how the furca may be released from the retinaculum.

Figure 13

Comparative transversal view of the 4th abdominal segment in *Orchesella cincta* reconstructed with MicroCT. A) Furca flexed, B) furca extended, C-D) schematic representation of the functioning of the jumping apparatus. C) Furca flexed, D) furca extended.

Figure 14

Schematic view of the functioning of the jumping apparatus in *Orchesella cincta*. A) Internal side view (flexed furca), B) Internal side view (flexed furca). The arrows show the direction of the muscle fibers.

Dvm: dorsoventral muscles, llm: lateral longitudinal muscles, isllm: intersegmental laterolongitudinal muscles, isdllm: intersegmental dorsolongitudinal muscles, dlm: dorsal longitudinal muscles, istm: intersegmental transversal muscle.

Figure 15

Schematic representation of the jumping apparatus in the flexed furca (A) and extended furca (B) phases in *Orchesella cincta*.